Inhibition of enolase: the crystal structures of enolase-Ca2(+)- 2-phosphoglycerate and enolase-Zn2(+)-phosphoglycolate complexes at 2.2-A resolution.

ARTICLE *in* BIOCHEMISTRY · APRIL 1991

Impact Factor: 3.02 · Source: PubMed

4 AUTHORS:

Lukasz Lebioda
University of South Carolina
140 PUBLICATIONS **3,051** CITATIONS
SEE PROFILE

Boguslaw Stec
114 PUBLICATIONS **3,667** CITATIONS
SEE PROFILE

John M Brewer
University of Georgia
97 PUBLICATIONS **1,989** CITATIONS
SEE PROFILE

Ewa Tykarska
Uniwersytet Medyczny im.Karola Marcinkows...
50 PUBLICATIONS **315** CITATIONS
SEE PROFILE

Inhibition of Enolase: The Crystal Structures of Enolase–Ca^{2+}–2-Phosphoglycerate and Enolase–Zn^{2+}–Phosphoglycolate Complexes at 2.2-Å Resolution[†,‡]

Lukasz Lebioda,*[,§] Boguslaw Stec,[§,∥] John M. Brewer,[⊥] and Ewa Tykarska[§,#]

Department of Chemistry, University of South Carolina, Columbia, South Carolina 29208, and Department of Biochemistry, University of Georgia, Athens, Georgia 30602

Received August 27, 1990; Revised Manuscript Received November 8, 1990

ABSTRACT: Enolase is a metalloenzyme which catalyzes the elimination of H_2O from 2-phosphoglyceric acid (PGA) to form phosphoenolpyruvate (PEP). Mg^{2+} and Zn^{2+} are cofactors which strongly bind and activate the enzyme. Ca^{2+} also binds strongly but does not produce activity. Phosphoglycolate (PG) is a competitive inhibitor of enolase. The structures of two inhibitory ternary complexes: yeast enolase–Ca^{2+}–PGA and yeast enolase–Zn^{2+}–PG, were determined by X-ray diffraction to 2.2-Å resolution and were refined by crystallographic least-squares to R = 14.8% and 15.7%, respectively, with good geometries of the models. These structures are compared with the structure of the precatalytic ternary complex enolase–Mg^{2+}–PGA/PEP (Lebioda & Stec, 1991). In the complex enolase–Ca^{2+}–PGA, the PGA molecule coordinates to the Ca^{2+} ion with the hydroxyl group, as in the precatalytic complex. The conformation of the PGA molecule is however different. In the active complex, the organic part of the PGA molecule is planar, similar to the product. In the inhibitory complex, the carboxylic group is in an orthonormal conformation. In the inhibitory complex enolase–Zn^{2+}–PG, the PG molecule coordiantes with the carboxylic group in a monodentate mode. In both inhibitory complexes, the conformational changes in flexible loops, which were observed in the precatalytic complex, do not take place. The lack of catalytic metal ion binding suggests that these conformational changes are necessary for the formation of the catalytic metal ion binding site.

Yeast enolase (2-phospho-D-glycerate hydrolyase, EC 4.2.1.11) is a metal-activated metalloenzyme (Brewer, 1981; Wold, 1971) which catalyzes the only dehydration reaction in glycolysis. The enzyme as isolated is dimeric (Brewer & Weber, 1968), each subunit containing 1 mol of tightly bound divalent cation, normally Mg^{2+} (Brewer & Weber, 1966). The cation binding and removal are associated with changes in absorption, fluorescence, subunit interaction strength, and thermal stability, so the tightly bound cation is called "conformational" metal ion (Brewer & Weber, 1966).

With conformational metal ions bound, the subunits may bind 1 mol of substrate or competitive inhibitor each, but little catalysis occurs (Faller & Johnson, 1974; Faller et al., 1977). However, substrate or analogue binding permits binding of 1 additional mol of divalent cation (Faller et al., 1977). If the conformational metal ion is an "activating" metal ion, e.g., Mg^{2+} or Zn^{2+}, catalysis occurs; the rate of catalysis is controlled by the second, "catalytic" metal ion (Brewer & Collins, 1980). If the conformational metal ion is a "nonactivating" metal ion, e.g., Ca^{2+}, no catalysis occurs.

The operational difference between activating and nonactivating metal ions is absolute in terms of reaction of two chromophoric substrate analogues (Brewer & Collins, 1980) and has been linked to a difference in preferred coordination geometry: activating conformational metal ions prefer or are relatively stable with octahedral complexes while the nonactivating metal ions tend either to have the low coordination number of 4 or to prefer higher coordination numbers of 7 or more (Brewer, 1985).

Crystallographic data for the binary complex enolase–Zn^{2+} have shown that the actual coordination of Zn^{2+} ions is trigonal bipyramidal (Lebioda & Stec, 1989) and so is the coordination of Mg^{2+} ions in the precatalytic complex enolase–Mg^{2+}–PGA. The substrate, PGA molecule, coordinates to the conformational metal ion with its hydroxylic oxygen (Lebioda & Stec, 1991). Both Zn^{2+} and especially Mg^{2+} have a strong preference for octahedral coordination when all ligands are oxygen atoms. It was proposed that the octahedral metal ion complexes would be too stable and substrate/product dissociation would be the rate-limiting factor (Lebioda & Stec, 1989). The present studies of the Ca^{2+} complex were undertaken to elucidate how nonactivating metal ions affect substrate binding. We have started the studies of enolase–Zn^{2+}–PG complex in hope that we will be able to find the catalytic metal ion binding site. Enolase crystals soaked in Zn^{2+} and PGA invariably cracked.

Materials and Methods

Crystals of yeast enolase suitable for X-ray diffraction studies were grown by vapor diffusion methods as described previously (Lebioda & Brewer, 1984). A solution containing equal volumes of 3% enolase, 2 mM Mg^{2+}, 1 mM EDTA, 1 mM dithiothreitol, 0.05 M citrate buffer (pH 5.0), and 55% saturated ammonium sulfate was equilibrated against a 55% saturated ammonium sulfate solution. The crystals were transferred to solutions of 75% saturated ammonium sulfate with 0.05 M citrate buffer, pH 6.0, gradually made in one

[†] This work was supported by the National Institutes of Health (Grant GM 34994).

[‡] The atomic coordinates for the structure of enolase–Ca^{2+}–2-phosphoglycerate have been deposited to the Brookhaven Protein Data Bank as entry 5ENL and for the structure of enolase–Zn^{2+}–phosphoglycolate as entry 6ENL.

[§] University of South Carolina.

[∥] Permanent address: SLAFIBS, Jagiellonian University, Cracow, Poland.

[⊥] University of Georgia.

[#] Permanent address: Department of Chemistry, University of Poznan, Poznan, Poland.

0006-2960/91/0430-2823$02.50/0

Table I: Summary of Parameters and Results of Restrained Refinement

	σ	final rms E-Ca^{2+}-PGA	final rms E-Zn^{2+}-PG
distances (Å)			
bond length (1–2 neighbors)	0.020	0.015	0.015
bond angles (1–3 neighbors)	0.040	0.044	0.045
planes (1–4 neighbors)	0.050	0.049	0.048
planar groups (Å)	0.020	0.011	0.011
chiral vol (Å^3)	0.150	0.146	0.145
nonbonded contacts (Å)			
single-torsion contacts	0.45	0.20	0.20
multiple-torsion contacts	0.45	0.21	0.24
possible H-bonding contacts	0.45	0.24	0.27
torsion angles (deg)			
peptide plane (ω)	3.0	2.0	2.0
staggered (±60°, 180°)	12.0	18.2	18.4
orthonormal (±90°)	16.0	31.3	31.5
wt for diffraction data A, B, $s = A - B(\sin\theta/\lambda - {}^1/_6)$		7, −38	5.2, −32
final R (%)		14.8	15.7
Luzzati estimate of coordinates error (Å)		0.18	0.20
no. of water molecules in model		355	343

soaking experiment 20 mM Ca^{2+} and 20 mM PGA, in the other 20 mM Zn^{2+} and 20 mM phosphoglycolate. The crystals were resistant to the mother liquor changes; unit cell dimensions $a = b = 124.1$ Å and $c = 66.9$ Å were the same, within experimental error, as the native crystals. The data were collected with a Xentronic area detector with a crystal to detector distance of 16 cm and a swing angle of −25.0° and processed by using the XENGEN software. For an enolase–Ca^{2+}–PGA complex crystal, 55 111 reflections were merged and yielded 25 514 symmetry-independent reflections with R_{int} = 6.9%; 20 697 reflections with $F > 3\sigma(F)$ and at a resolution better than 8 Å were used in the structure refinement. For an enolase–Zn^{2+}–phosphoglycolate crystal, 51 668 reflections were measured and yielded 25 431 reflections with R_{int} = 8.7%; 18 279 reflections with $F > 3\sigma(F)$ and at a resolution better than 8 Å were used in the structure refinement.

The structure of the binary complex enolase–Zn^{2+}, which was determined at 1.9-Å resolution and refined to 14.9% (Lebioda & Stec, 1989), was used as the starting model with the metal ion coordination sphere omitted. This model was a very good staring point, yielding R = 23% and 25% for Ca^{2+} and Zn^{2+} complexes, respectively. The metal ions and ligand molecules were positioned in the electron density maps calculated prior to their inclusion in the refinement. The shape of ligand electron densities remained essentially unchanged during refinement. The dictionary for the ligand molecules was constructed by using the bond lengths and bond angles found in the crystal structure of trisodium 2-phospho-D-glycerate hexahydrate (Lis, 1985). No restraints on the torsion angles of the substrate molecule were applied. The structure refinements by restrained least-squares were carried out by using the PROLSQ program (Hendrickson & Konnert, 1980). The final values of the refinement parameters are given in Table I and the distributions of R factor in Table II. Figure 1 represents the Ramachandran plot for the enolase–Ca^{2+}–

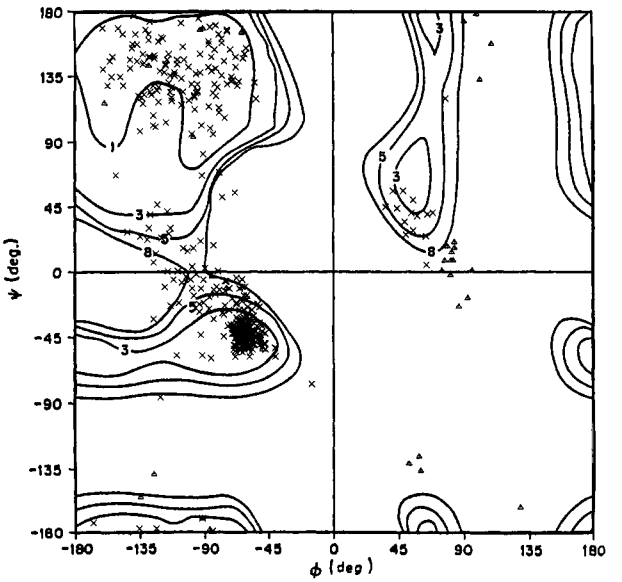

FIGURE 1: Ramachandran plot for the enolase–Ca^{2+}–PGA complex. Conformational angles for non-glycine residues are marked with crosses and for glycine residues with triangles. The superimposed iso-energy levels correspond to an alanine tripeptide. The energy contours in given intervals expressed kilocalories per mole (1 cal = 4.184 J) are shown.

PGA structure superimposed on the conformational energy map for alanine tripeptides (Brant & Schimmel, 1967). A corresponding plot for the enolase–Zn^{2+}–phosphoglycolate structure is very similar (not shown). A more detailed analysis of the geometry of the enolase molecule can be found in our previous paper (Stec & Lebioda, 1990). Plots of average isotropic temperature factors as a function of residue numbers are shown in Figure 2. For both structures, these plots are almost identical; this reflects the very close similarity of both structures.

RESULTS

The location of the active site is shown in Figure 3, taken from Lebioda and Stec (1991). The electron density found as a result of PGA binding to the enolase–Ca^{2+} complex is shown in Figure 4. Three lobes are apparent. The assignment of the phosphate moiety to the lobe at Arg374 is quite obvious. The lobe is large with spherical density and is the highest peak in the map. This location is also the sulfate ion binding site in the native enolase structure (Stec & Lebioda, 1990) and the phosphate binding site in the enolase–Mg^{2+}–PGA/PEP complex (Lebioda & Stec, 1991). The electron density lobe at the Ca^{2+} ion is strong and spherical. Its shape and density are similar to those of the strongly bound water also at the Ca^{2+} ion (Figure 5) and correspond well to a hydroxyl group. Modeling the PGA molecule with the carboxylate group in this density, either as a monodentate or as a bidentate ligand, led to a poor fit with one or both oxygen atoms out of the electron density. Also, with the position of the phosphate group well-defined, the chiral C2 atom had to be placed outside the electron density. Thus, the coordination of the PGA molecule through its hydroxyl group to the Ca^{2+} ion appears to be dominating.

Table II: Number of Reflections with $F > 3\sigma(F)$ and R Factors as a Function of Resolution for (I) Enolase–Ca^{2+}–PGA and (II) Enolase–Zn^{2+}–PA Complexes

D_{min} (Å)	8–4.5	3.5	3.0	2.8	2.6	2.4	rest	total
I, no. of reflections	2250	3169	3460	2047	2591	3291	3894	20697
I, R (%)	18.1	12.5	14.0	14.8	15.3	15.1	15.6	14.8
II, no. of reflections	2493	3260	3393	1911	2259	2559	2412	18279
II, R (%)	17.5	13.3	15.0	16.1	17.0	17.1	17.7	15.7

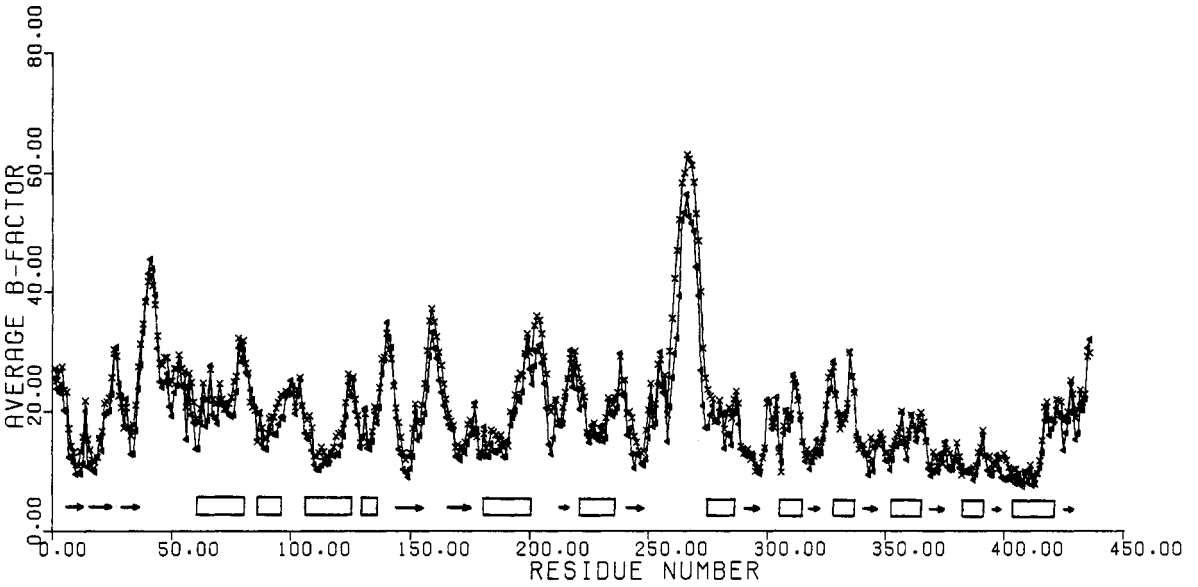

FIGURE 2: Average temperature factor plotted against the residue number. Triangles are for the Ca^{2+} complex and crosses for the Zn^{2+} complex. The secondary structure elements are marked below, arrows corresponding to β-strands and rectangles to α-helices.

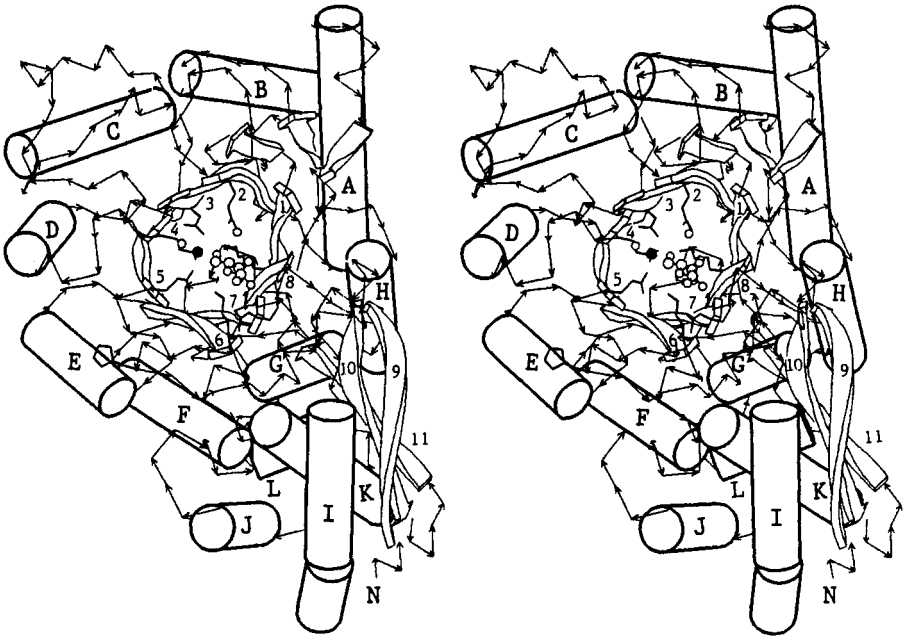

FIGURE 3: Stereoview of enolase seen approximately along the barrel axis. The active site is located in the deep cavity at the carboxylic end of the barrel. The position of the conformational metal ion is marked with a filled circle. The PGA molecule and two water molecules in the active site are drawn with open circles. The main secondary structure elements are denoted according to the previous notation (Lebioda et al., 1989). The sequence of secondary structure elements along the peptide chain is N-9, 10, 11, I, J, K, L, 1, 2, A, B, 3, C, 4, D, 5, E, 6, F, 7, G, 8, and H–COOH. The side chains of the active-site residues are drawn as stick models. From β-strand: 2 branches, Glu168; 3, Asp246; 4, Glu295; 5, Asp320; 6, Lys345; 7, Arg374; and 8, Lys396.

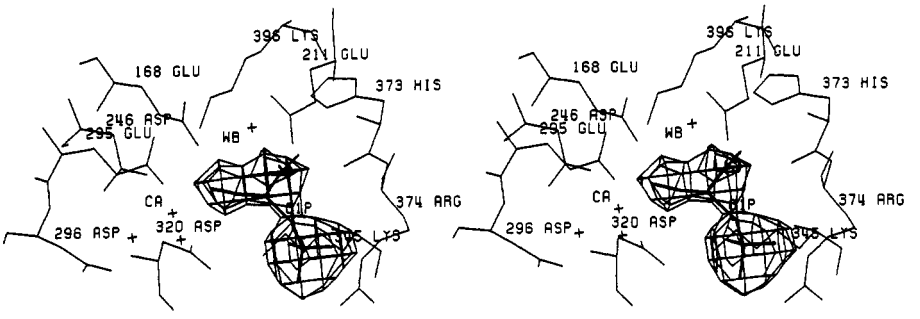

FIGURE 4: Active site in the enolase–Ca^{2+}–PGA complex. The electron density, from a difference Fourier map contoured at the 2.0σ level, indicates that the carboxylic group is perpendicular to the plane of the carbon atoms. The water molecule postulated as the base in the precatalytic complex, WB, is not in a position to interact with the proton on C(2), and neither is Glu168. The temperature factors for the PGA molecule are in a 40–44-Å^2 range, for the active-site residues in a 10–20-Å^2 range.

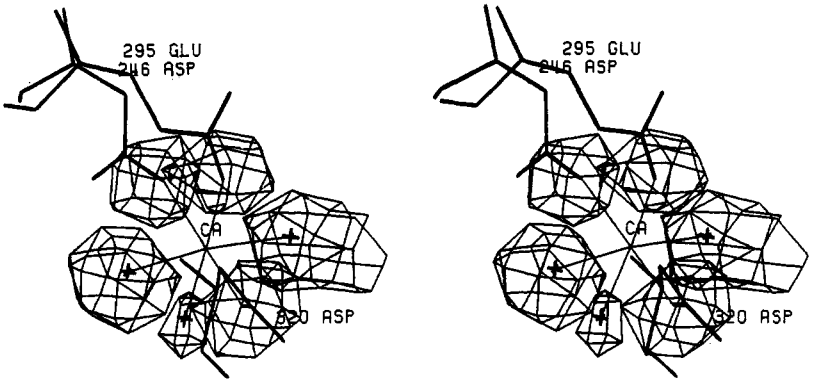

FIGURE 5: Coordination of the Ca^{2+} ion. The electron density, contoured at the 2.2σ level, is from a difference Fourier map. The atoms coordinated to the Ca^{2+} ion were omitted from the model. The ligands form an almost regular octahedron.

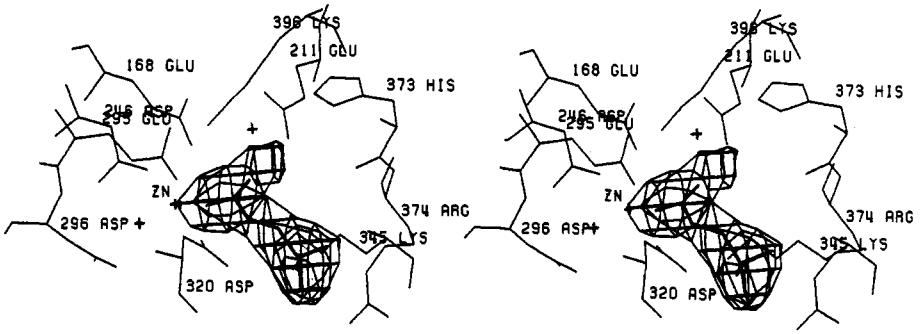

FIGURE 6: Active site in the enolase–Zn^{2+}–PG complex. The inhibitor molecule binds to the metal ion with one of the oxygen atoms. The coordination of Zn^{2+} is trigonal bipyramidal, as it is in the binary complex. The electron density, contoured at the 2.5σ level, is from an omit difference Fourier map. The temperature factors for the inhibitor are in a 37–40-Å^2 range, for the active-site residues in a 10–20-Å^2 range.

The third lobe is relatively short and broadened at the end. It corresponds well to the carboxylic group of the PGA molecule in a conformation similar to that found in the structure of its potassium salt (Lis, 1985), with the carboxylic group perpendicular to the plane of the carbon atoms. This is in contrast with the conformation found in the precatalytic complex enolase–Mg^{2+}–PGA/PEP where the carbon atoms and the oxygen atoms of the carboxylic group are coplanar (Lebioda & Stec, 1991).

The environment of the Ca^{2+} ion is octahedral with an additional water molecule coming in as the sixth ligand. The electron density for this water molecule is somewhat weaker, indicating perhaps greater mobility (Figure 5). The angles between the Ca^{2+} and the ligands show only small deviations from ideal octahedral geometry.

The enzyme conformation is essentially the same as in the binary complex, enolase–Zn^{2+}. The loop movement observed in the precatalytic ternary complex (Lebioda & Stec, 1991) was not found here. We did not find electron density in the difference Fourier maps which could be interpreted as coming from the catalytic metal ion.

The electron density corresponding to the phosphoglycolic acid bound in the active site is shown in Figure 6. It is apparent that the molecule is bound to the Zn^{2+} ion with the carboxylic group in a monodentate fashion. Thus, in the absence of a hydroxyl available for binding to the Zn^{2+} ion, the carboxyl fills in. There is some electron density extending from the noncoordinated oxygen atom of the carboxylic group. At a slightly higher contouring level, 3σ, this density disappears. Its interpretation is not obvious; perhaps some PG molecules binds in the same mode as PGA molecules, with the carboxylate toward Lys396.

The metal ion coordination is trigonal bipyramidal, as it is in the binary complex (Lebioda & Stec, 1989). The enzyme conformation also remains essentially unchanged from the binary complex. There is no movement of flexible loops observed in the precatalytic complex. Again, there was no electron density that could be assigned to the catalytic metal ion.

Discussion

The crystallographic data show two modes of nonproductive binding by enolase. In the Ca^{2+} complex, the substrate molecule, PGA, binds in the orthonormal conformation. In the active, precatalytic complex, the conformation is coplanar, resembling the product, PEP molecule (Lis, 1987), and presumably also the transition state.

There are two possible origins of this difference. First, the carboxylate ligands of the conformational metal ion are rigidly held by the protein so the Ca^{2+} site is outward about 0.3 Å from the Zn^{2+} site. This is in agreement with the ionic radii difference (0.99 and 0.74 Å, respectively) and leads to a position of the oxygen atom of the hydroxyl that is different by twice the difference in ionic radii, 0.5 Å. Apparently, it is too much to accommodate by the active site, and the whole substrate molecule binds in a nonproductive manner.

The second contributing factor is the polarization of the substrate hydroxyl. The Ca^{2+} ion, due to its larger ionic radius and coordination number, should induce weaker polarization than the smaller Mg^{2+} ion with an ionic radius of 0.65 Å. The importance of this factor is underlined by the observation that the enolase–Cd^{2+} complex has 10% of the activity of the enolase–Mg^{2+} complex (Spencer & Brewer, 1984). The ionic radius of Cd^{2+} is 0.97 Å, very similar to Ca^{2+}, but as a transition-metal ion, Cd^{2+} should induce stronger polarization. It may be speculated further that the polarized hydroxyl of the PGA molecule forms an intramolecular hydroxyl bond to the carboxylic group, thus stabilizing the coplanar conformation observed in the precatalytic complex. One way of checking this hypothesis would be to determine the structure

of the inhibitory complex between enolase–Mg^{2+}–tartronate semialdehyde phosphate (TSP). In TSP, the hydroxyl is replaced by the aldehydic oxygen atom which cannot donate a hydrogen bond (Spring & Wold, 1971).

The structure of the ternary complex enolase–Zn^{2+}–phosphoglycolate shows another mode of inhibitory ligand binding. The nonproductive binding is in agreement with the data showing that yeast enolase does not catalyze the exchange of protons of phosphoglycolate while rabbit muscle enolase does (Stubbe & Abeles, 1980).

The most interesting observation is that despite the presence of 20 mM Zn^{2+} there is no indication of the presence of the metal ion bound in the catalytic site. It has been shown that the catalytic metal ion (Mg^{2+}) binds to the enzyme at pH 7.8 in the presence of PG (Brewer, 1971). Such binding is associated with changes in fluorescence and absorption of the enzyme (Brewer, 1971). Admittedly, the high ionic strength in the crystals and the low pH (6 rather than 7.8) could weaken binding, but under the same conditions, if PGA is used instead of PG, the crystals shatter immediately. We think, therefore, that the conformational transition, the onset of which was observed in the precatalytic ternary complex and which is not observed in the two inhibitory complexes, is crucial for the formation of the catalytic metal ion binding site.

ACKNOWLEDGMENTS

We thank M. Deacon and E. M. Westbrook for help with the data collection at the Midwest Area Diffractometer Facility.

REFERENCES

Brant, D. A., & Schimmel, P. R. (1967) *Proc. Natl. Acad. Sci. U.S.A. 58*, 428–435.
Brewer, J. M. (1971) *Biochim. Biophys. Acta 250*, 251–257.
Brewer, J. M. (1981) *CRC Crit. Rev. Biochem. 11*, 209–254.
Brewer, J. M. (1985) *FEBS Lett. 182*, 8–14.
Brewer, J. M., & Weber, G. (1966) *J. Biol. Chem. 241*, 2550–2557.
Brewer, J. M. & Weber, G. (1968) *Proc. Natl. Acad. Sci. U.S.A. 59*, 216–223.
Brewer, J. M., & Collins, K. M. (1980) *J. Inorg. Biochem. 13*, 151–164.
Faller, L. D., & Johnson, A. M. (1974) *Proc. Natl. Acad. Sci. U.S.A. 71*, 1083–1087.
Faller, L. D., Baroudy, B. M., Johnson, A. M., & Ewall, R. X. (1977) *Biochemistry 16*, 3864–3869.
Hendrickson, W. A., & Konnert, J. H. (1980) in *Biomolecular Structure, Function, Conformation and Evolution* (Srinivasan, R., Ed.) pp 43–57, Pergamon Press, Oxford.
Lebioda, L., & Brewer, J. M. (1984) *J. Mol. Biol. 180*, 213–215.
Lebioda, L., & Stec, B. (1989) *J. Am. Chem. Soc. 111*, 8511–8513.
Lebioda, L., & Stec, B. (1991) *Biochemistry* (preceding paper in this issue).
Lis, T. (1985) *Acta Crystallogr. C41*, 1578–1580.
Lis, T. (1987) *Acta Crystallogr. C43*, 1898–1900.
Nowak, T., Mildvan, A. S., & Kenyon, G. L. (1973) *Biochemistry 12*, 1690–1701.
Spencer, S. G., & Brewer, J. M. (1984) *J. Inorg. Biochem. 20*, 39–52.
Spring, T. G., & Wold, F. (1971) *Biochemistry 10*, 4649–4654.
Stec, B., & Lebioda, L. (1990) *J. Mol. Biol. 24*, 235–248.
Stubbe, J. A., & Abeles, R. H. (1980) *Biochemistry 19*, 5505–5512.
Wold, F. (1971) *Enzymes (3rd Ed.) 5*, 499–538.

Identification of the Disulfide Bonds of Human Complement C1s†

Daniel Hess, Johann Schaller, and Egon E. Rickli*
Institute of Biochemistry, University of Bern, Freiestrasse 3, CH-3012 Bern, Switzerland
Received June 21, 1990; Revised Manuscript Received October 22, 1990

ABSTRACT: C1s, one of the three subcomponents of C1, the first component of the complement system, is a complex serine protease. To determine the disulfide-bonding pattern, fragments of C1s were generated by cleavage with pepsin, thermolysin, or subtilisin. Disulfide bonds have been identified by several methods, for example, direct observation of the phenylthiohydantoin derivative of cystine during Edman degradation of isolated peptides and placement in the known cDNA sequence. All of the 26 half-cystines are linked in disulfide bonds occurring at positions 50–68, 120–132, 128–141, 143–156, 160–187, 219–236, 279–326, 306–339, 344–388, 371–406, 410–534, 580–603, and 613–644. All of the disulfide bonds of the earlier described substructures of C1s, the EGF-homologous part, the two SCR units, and the two domains typical for C1s and C1r are localized within these domains.

The first component of the classical complement pathway, C1,[1] is a complex proteinase with C1q as the recognition unit and a catalytic unit consisting of a Ca^{2+}-dependent tetrameric complex of two homologous serine proteases, C1r and C1s. Binding of C1 to various immunocomplexes or nonimmune activators is mediated by C1q and leads to activation of the catalytic subunit by a two-step process. Initially the active form of C1r is generated by an autocatalytic process, which then activates C1s to $\overline{C1s}$, the proteolytic enzyme that finally triggers the classical pathway [reviewed by Cooper (1985) and Schumaker et al. (1987)].

† This work was supported by Grant 31-8694.86 of the Swiss National Science Foundation.
* Author to whom correspondence should be addressed.

[1] Abbreviations: RP-HPLC, reversed-phase high-performance liquid chromatography; ABI-sequencer, Applied Biosystems protein sequencer 477A; SBD-F, ammonium 7-fluorobenz-2-oxa-1,3-diazole-4-sulfonate; TFA, trifluoroacetic acid; Cys, half-cystine. The nomenclature of complement components is used as recommended by the World Health Organization; activated components are indicated by a superscripted bar.

0006-2960/91/0430-2827$02.50/0